frontiers in Astronomy and Space Sciences

ORIGINAL RESEARCH
published: 17 October 2017
doi: 10.3389/fspas.2017.00023

Statistical Detection of the He II Transverse Proximity Effect: Evidence for Sustained Quasar Activity for >25 Million Years

Tobias M. Schmidt[1,2]*, *Gabor Worseck*[2], *Joseph F. Hennawi*[1,2], *J. Xavier Prochaska*[3], *Neil H. M. Crighton*[4], *Zarija Lukić*[5] *and Jose Oñorbe*[2]

[1] Department of Physics, University of California, Santa Barbara, Santa Barbara, CA, United States, [2] Max-Planck-Institut für Astronomie, Heidelberg, Germany, [3] Department of Astronomy and Astrophysics, UCO/Lick Observatory, University of California, Santa Cruz, Santa Cruz, CA, United States, [4] Centre for Astrophysics and Supercomputing, Swinburne University of Technology, Melbourne, VIC, Australia, [5] Lawrence Berkeley National Laboratory, Berkeley, CA, United States

The reionization of helium at $z \sim 3$ is the final phase transition of the intergalactic medium and supposed to be driven purely by quasars. The He II transverse proximity effect—enhanced He II transmission in a background sightline caused by the ionizing radiation of a foreground quasar—therefore offers a unique opportunity to probe the morphology of He II reionization and to investigate the emission properties of quasars, e.g., ionizing emissivity, lifetime and beaming geometry. We use the most-recent *HST*/COS far-UV dataset of 22 He II absorption spectra and conduct our own dedicated optical spectroscopic survey to find foreground quasars around these He II sightlines. Based on a set of 66 foreground quasars, we perform the first statistical analysis of the He II transverse proximity effect. Despite a large object-to-object variance, our stacking analysis reveals an excess in the average He II transmission near the foreground quasars at 3σ significance. This statistical evidence for the transverse proximity effect is corroborated by a clear dependence of the signal strength on the inferred He II ionization rate at the background sightline. Our detection places, based on the transverse light crossing time, a geometrical limit on the quasar lifetime of $t_Q > 25$ Myr. This evidence for sustained activity of luminous quasars is relevant for the morphology of H I and He II reionization and helps to constrain AGN triggering mechanisms, accretion physics and models of black hole mass assembly. We show how future modeling of the transverse proximity effect can additionally constrain quasar emission geometries and e.g., clarify if the large observed object-to-object variance can be explained by current models of quasar obscuration.

Keywords: dark ages, reionization, first stars – intergalactic medium, – quasars: general, – quasars: lifetime, – quasars: obscuration

OPEN ACCESS

Edited by:
Mauro D'Onofrio,
Università degli Studi di Padova, Italy

Reviewed by:
José María Solanes,
University of Barcelona, Spain
Milan S. Dimitrijevic,
Astronomical Observatory, Serbia

***Correspondence:**
Tobias M. Schmidt
tschmidt@mpia.de

Specialty section:
This article was submitted to Milky Way and Galaxies, a section of the journal Frontiers in Astronomy and Space Sciences

Received: *01 September 2017*
Accepted: *29 September 2017*
Published: *17 October 2017*

Citation:
Schmidt TM, Worseck G, Hennawi JF, Prochaska JX, Crighton NHM, Lukić Z and Oñorbe J (2017) Statistical Detection of the He II Transverse Proximity Effect: Evidence for Sustained Quasar Activity for >25 Million Years. Front. Astron. Space Sci. 4:23. doi: 10.3389/fspas.2017.00023

1. INTRODUCTION

The double ionization of helium, known as He II reionization, marks the final phase transition of the intergalactic medium (IGM) and is closely related to the emission properties of the quasar population that is supposed to drive He II reionization. Hydrogen, according to the currently accepted picture (Haardt and Madau, 2012; Planck Collaboration et al., 2016), was reionized

at redshifts $z \sim 8$ primarily by the UV photons from stars. However, stellar spectra are not hard enough to supply sufficient numbers of photons with energies >4 Ry, required to doubly ionize helium. He II reionization therefore took place much later, when quasars became sufficiently abundant, culminating in the completion of helium reionization at $z \approx 2.7$ (Madau and Meiksin, 1994; Reimers et al., 1997; Miralda-Escudé et al., 2000; Faucher-Giguère et al., 2009; McQuinn, 2009; Worseck et al., 2011; Haardt and Madau, 2012; Compostella et al., 2013, 2014; Worseck et al., 2016). In the general picture of He II reionization, quasars create photoionized bubbles in the IGM which expand with time and eventually overlap, leading to the present day situation that the IGM is kept in photoionization equilibrium and highly ionized by a homogeneous and uniform UV background (Bolton et al., 2006; Furlanetto and Oh, 2008; McQuinn, 2009; Furlanetto and Dixon, 2010; Furlanetto and Lidz, 2011; Haardt and Madau, 2012; Meiksin and Tittley, 2012; Compostella et al., 2013, 2014; Davies et al., 2017). Since quasars are rare but bright sources, the reionization process is rather patchy and inhomogeneous. Its morphology therefore contains extensive information about the emission properties of the quasars.

At redshift $z \sim 3$, the $\lambda_{\rm rest} = 304$ Å He II Lyα transition is redshifted sufficiently into the far-UV (FUV) to be observable with space based telescopes, in particular the Hubble Space Telescope (*HST*). The usual technique is to take FUV spectra of background quasars and infer the helium ionization characteristics along the sightline from the absorption properties of the He II Lyα forest. The presence of a foreground quasar close to such a He II sightline allows to explore the effect of the foreground quasars ionizing radiation on the helium ionization state along the background sightline.

Figure 1 illustrates the prototype sightline of such a constellation. The bottom panel shows a Space Telescope Imaging Spectrograph (*HST*/STIS) FUV spectra (Heap et al., 2000) along the sightline toward the background quasars Q 0303−003. It shows over large regions Gunn-Peterson troughs (Gunn and Peterson, 1965) of saturated He II Lyα absorption, very similar to hydrogen Lyα spectra of high-redshift $z > 6$ quasars. Substantial He II transmission is only observed close to the background quasar, the so called line of sight proximity region. Here, the ionizing radiation from the background quasar has already sufficiently ionized helium to allow high He II transmission. In addition, the spectrum shows a striking transmission spike at $z = 3.05$. At the same redshift and with a separation of $\Delta\theta = 6'$ from the background sightline Jakobsen et al. (2003) found a foreground quasar and established the picture on the He II transverse proximity effect. In this picture, the foreground quasar photoionizes its surrounding and the background sightline intersects this ionization bubble, leading to strong He II transmission at the position of the foreground quasar.

Observing a strong transverse proximity effect in such a constellation allows to infer a geometric limit on the age of the quasar. Since one observed the quasar and the enhanced He II transmission at the same redshift and therefore same lookback time, the quasar has to already shine for at least the transverse light crossing time to give the photons enough time to reach the background sightline. This constellation might also give

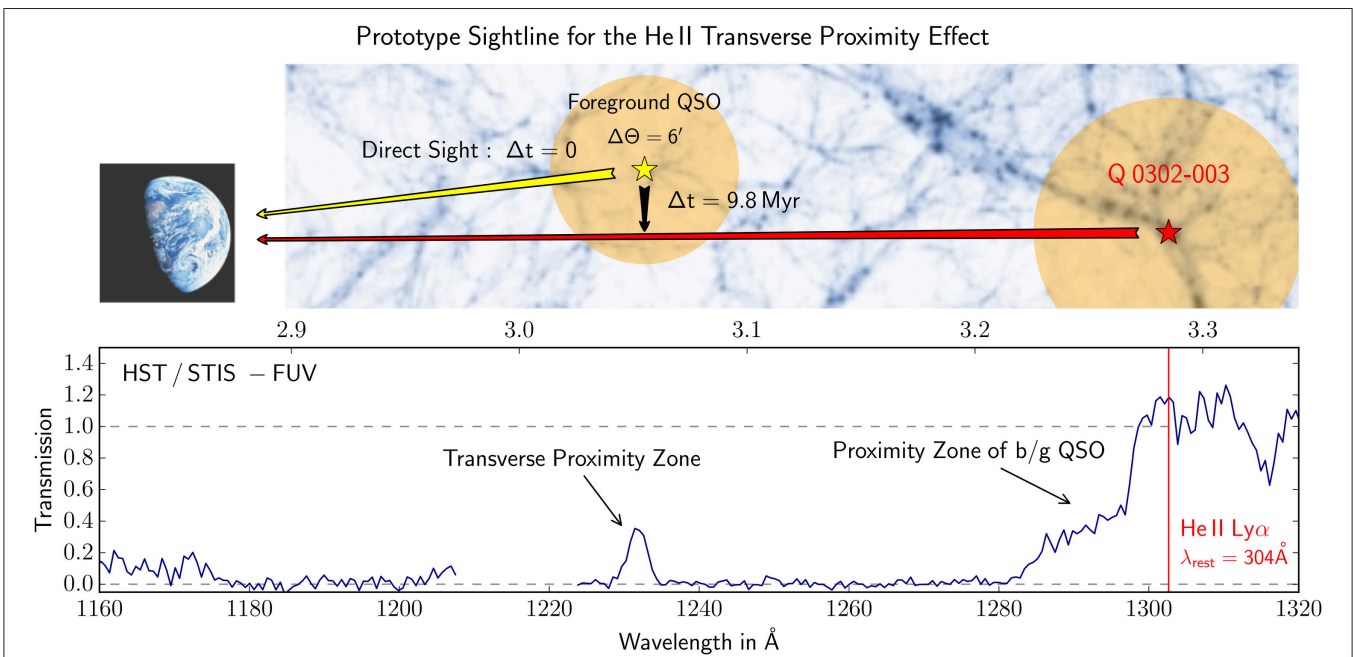

FIGURE 1 | This illustration shows the basic concept of the He II transverse proximity effect using the example of the Q 0302−003 prototype sightline. The bottom panel shows the *HST*/STIS FUV spectra from Heap et al. (2000), exhibiting an extended line of sight proximity effect close to the background sightline and a strong transmission peak at $z = 3.05$, caused by the proximity region of a close-by foreground quasar (Jakobsen et al., 2003). This constellation allows to derive a geometrical constraint on the age of the foreground quasar, based on the transverse light crossing time.

insights into the quasar emission geometry. The foreground quasar appears as unobscured Type I from Earth but its effect on the background sightline crucially depends on the obscuration properties toward the background sightline.

This illustrates the unique abilities to infer quasar properties offered by the He II transverse proximity effect. However, up to now, the Q 0302−003 sightline represents the only strong detection of a He II transverse proximity effect. Our aim is therefore to expand the sample, find additional foreground quasars close to He II sightlines and conduct a systematic investigation of the He II transverse proximity effect.

2. DEDICATED HELIUM REIONIZATION SURVEY

To increase the data sample and facilitate a statistical analysis of helium reionization, we are performing a comprehensive helium reionization survey. This includes the discovery and observation of new He II sightlines and a homogeneous and extremely careful reduction of all existing *HST* observations presented in Worseck et al. (2016). In addition, we conducted a dedicated optical foreground quasar survey around the 22 available He II sightlines which is described in Schmidt et al. (2017) and shall be summarized in the following.

The foreground quasar survey consists of a deep narrow survey conducted on 8 m class telescopes covering the immediate vicinity of the He II sightline and a wider survey targeting individual quasars on 4 m telescopes. The deep survey covers separations from the He II sightline up to $\Delta\theta \leq 10'$ and reaches a limiting magnitude of $r \leq 23.5$ mag. Quasar candidates were selected using deep multi-color imaging, primarily obtained with the Large Binocular Cameras at the Large Binocular Telescope (LBT/LBC, Giallongo et al., 2008; Speziali et al., 2008). The main concern here was to reach a *U*-band limiting magnitude of ≈ 26 mag. For spectroscopic confirmation the VIsible MultiObject Spectrograph (VIMOS, Le Fèvre et al., 2003) at the Very Large Telescope (VLT) was used. To find foreground quasars with larger separations from the background sightline, which are in particular important to probe long quasar lifetimes, we conducted a wide but shallower survey on 4 m class telescopes. We selected candidates from public quasar catalogs (DiPompeo et al., 2015; Richards et al., 2015) which are based on optical imaging (SDSS) and mid-infrared photometry from the *Wide-field Infrared Survey Explorer* (*WISE,* Wright et al., 2010). Using the *WISE* 3.6 and 4.5 μm bands allow very efficient quasar selection (Stern et al., 2012; Assef et al., 2013). Spectroscopic confirmation was done with the European Southern Observatory 3.5 m New Technology Telescope Faint Object Spectrograph and Camera (NTT/EFOSC2, Buzzoni et al., 1984) and the Calar Alto Observatory (CAHA) 3.5 m telescope TWIN spectrograph within 37 nights between November 2014 and August 2015. The wide survey reaches down to $r \leq 21.5$ mag and extends out to $\Delta\theta \approx 90'$ in case the quasar candidates were bright enough to expect a measurable effect on the background sightline.

In total, our surveys discovered 121 new quasars. We complement this sample by selecting quasars from the literature and in particular the spectroscopic catalogs of the Sloan Digital Sky Survey (SDSS, York et al., 2000) and the Baryon Oscillation Spectroscopic Surveys (BOSS, Eisenstein et al., 2011;

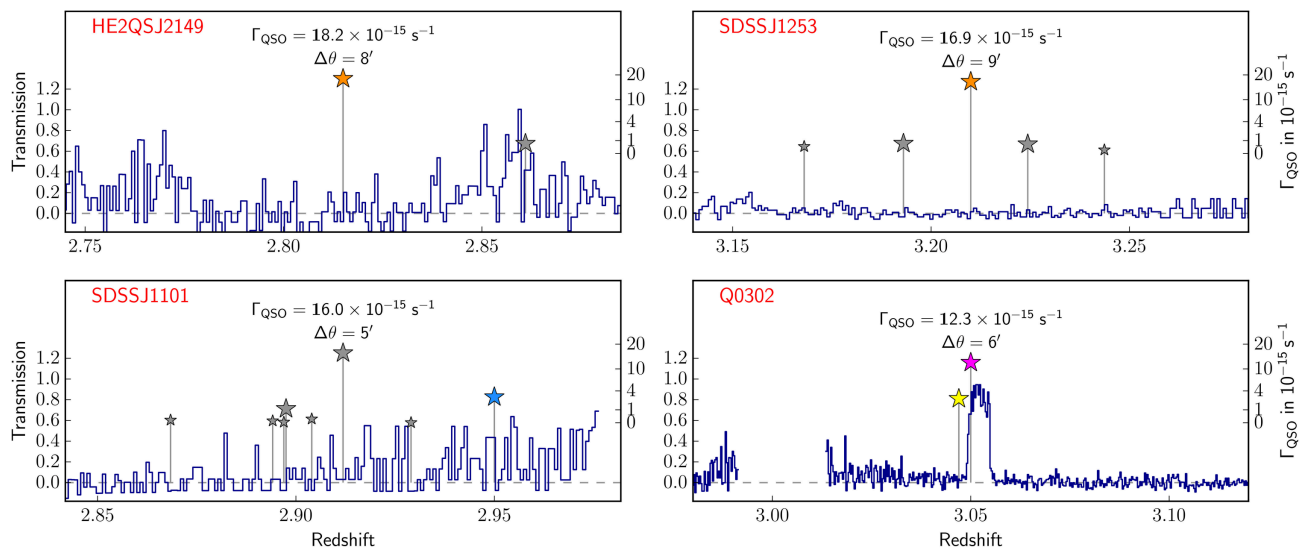

FIGURE 2 | He II spectra in the vicinity of the four foreground quasars with the highest estimated He II ionization rate Γ^{HeII}_{QSO} from Schmidt et al. (2017). Colors indicate the origin of the objects. (yellow: VLT/VIMOS; orange: CAHA/TWIN; blue: ESO NTT/EFOSC2; gray: SDSS/BOSS; pink: Literature). Size and vertical displacement of star symbols represent He II ionization rate. Only the previously known quasar along the Q 0302−003 sightline (Jakobsen et al., 2003) is associated with a strong He II transmission peak. The other three objects show, despite their up to 50% higher He II ionization rate and comparable other properties, extremely low He II transmission along the background sightline. One could speculate that these objects might be either very young or highly obscured toward the background sightline. ©: AAS. Figure reproduced from Schmidt et al. (2017).

Dawson et al., 2013) twelfth data release (Alam et al., 2015; Pâris et al., 2016). For all objects we calculate the estimated He II photoionization rate at the background sightline $\Gamma^{\rm HeII}_{\rm QSO}$ assuming isotropic emission, infinite quasar lifetime and no IGM absorption. For details see Schmidt et al. (2017). Our sample contains 66 foreground quasars for which we have full spectral coverage along the background sightline and which exceed $\Gamma^{\rm HeII}_{\rm QSO} > 0.5 \times 10^{-15}\,{\rm s}^{-1}$. For comparison, the He II UV background at $z \sim 3$ should be approximately $\Gamma^{\rm HeII}_{\rm UVB} \approx 1 \times 10^{-15}\,{\rm s}^{-1}$(Faucher-Giguère et al., 2009; Haardt and Madau, 2012; Khrykin et al., 2016).

3. THE TRANSVERSE PROXIMITY EFFECT OF INDIVIDUAL QUASARS

For the prototype object at $z = 3.05$ along the Q 0302−003 sightline we calculate an expected ionization rate of $\Gamma^{\rm HeII}_{\rm UVB} \approx 12 \times 10^{-15}\,{\rm s}^{-1}$. Thus, this object should exceed the He II UV background by approximately one order of magnitude. Observing a strong transverse proximity effect is therefore not surprising. Within our study we find three other foreground quasars that should cause up to 50% higher He II ionization rates at the background sightlines. The He II spectra associated with all four of these objects are shown in **Figure 2**. Surprisingly, the three new objects show no evidence for strong transverse proximity effect. On the contrary, we find completely ordinary and in several cases even fully saturated He II absorption. The three new foreground quasars are in terms of luminosity, separation from the background sightline and redshift comparable to the prototype quasar. It is therefore rather unexpected to find not even the slightest indication of a transverse proximity effect for any of them.

Possible explanations are that these quasars might be too young and therefore the ionizing radiation had not enough time to reach the background sightline. Given the transverse separations, this would point toward quasar ages below 8–15 Myr. Another possible explanation would be quasar obscuration. According to the common quasar unification models (e.g., Antonucci, 1993; Elvis, 2000), the dichotomy between Type I and Type II quasars is purely an orientation effect. Each quasar should emit only toward some part of the sky, approximately 50% according to (e.g., Brusa et al., 2010; Lusso et al., 2013; Marchesi et al., 2016), and be obscured toward the other directions. However, it seems quite unlikely that three out of four quasars are oriented in a way that no ionizing radiation at all reaches the background sightline. Without further investigation it therefore remains purely speculative why we find no strong transverse proximity effect for the three strongest foreground quasars.

4. STATISTICAL DETECTION OF THE TRANSVERSE PROXIMITY EFFECT

Apart form the non-detection of the proximity effect for individual quasars, we search for statistical evidence in the average He II transmission profile around foreground quasars. We therefore select foreground quasars with $\Gamma^{\rm HeII}_{\rm QSO} > 2 \times 10^{-15}\,{\rm s}^{-1}$ and stack the He II spectra on the positions of these foreground quasars. The result is shown in **Figure 3**, top panel. Despite the large scatter, we find a clear enhancement in the average He II transmission right at the location of the foreground quasars. We conduct a Monte Carlo analysis by stacking the He II spectra on random positions and find a significance of 3.1 σ for the measured transmission enhancement. In addition, we show in Schmidt et al. (2017) that the strength of this transmission enhancement roughly scales with the ionization rate of the foreground quasars and vanishes for $\Gamma^{\rm HeII}_{\rm QSO} < 2 \times 10^{-15}\,{\rm s}^{-1}$ which is roughly comparable to the He II UV background (Faucher-Giguère et al., 2009; Haardt and Madau, 2012). We are therefore confident that the observed effect is actually caused by the ionizing radiation of the foreground quasars.

Based on this statistical detection of the He II transverse proximity effect we can investigate the quasar lifetime. Therefore,

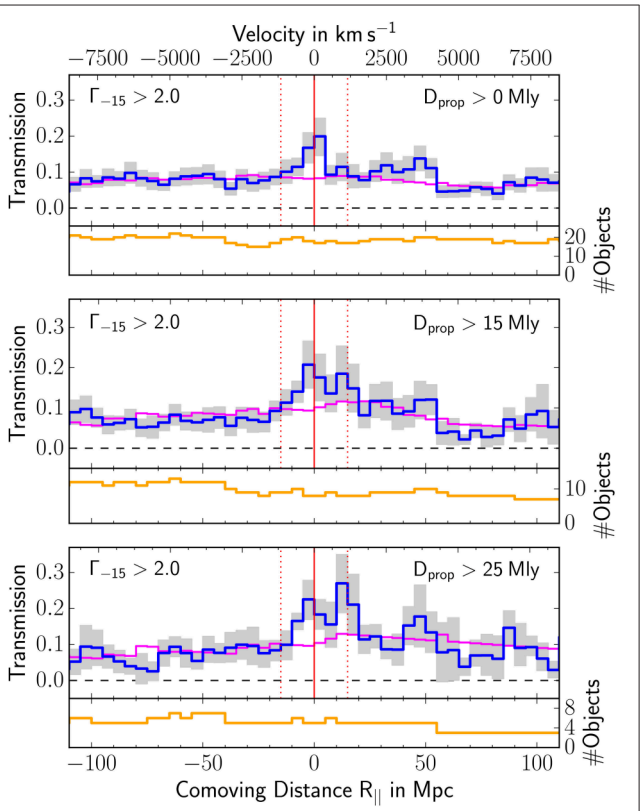

FIGURE 3 | Statistical detection of the He II transverse proximity effect from Schmidt et al. (2017). We compute an average He II transmission profile in the vicinity of the foreground quasars (blue) by stacking the He II spectra on the positions of known foreground quasars. Bootstrap errors are given in gray, the number of contributing objects in yellow. The purple line shows a simple model for the average He II transmission in the IGM. The top plot includes all quasars with $\Gamma^{\rm HeII}_{\rm QSO} > 2 \times 10^{-15}\,{\rm s}^{-1}$ and shows a clear transmission enhancement at the position of the foreground quasars (red). The other two plots include only a subset of foreground quasars with a minimum separation from the background sightline larger than 15 and 25 Mlyr. The transmission enhancement persists in these stacks, setting a clear constraint on the age of the foreground quasars. ©: AAS. Figure reproduced from Schmidt et al. (2017).

we include only foreground quasars in the stack that have a given minimum separation from the background sightline. As shown in **Figure 3**, the transverse proximity effect persists in the average transmission profile even for quasars with separations $>$ 25 Mlyr. The significance of the He II transverse proximity effect in the $>$15 and $>$25 Mlyr stacks was determined to be 3.2 σ and 2.6 σ. Based on the transverse light crossing time we conclude that the quasars have to shine for at least 25 Myr.

5. SUMMARY AND OUTLOOK ON FUTURE MODELING ATTEMPTS

In Schmidt et al. (2017) we have described our dedicated foreground quasar survey around 22 He II sightlines and the discovery of 121 new quasars. With the addition of quasars from SDSS/BOSS we have composed a relatively large foreground quasar sample that allows for the first time a statistical analysis of the He II transverse proximity effect. By the means of a stacking analysis, we were able to find statistical evidence for the presence of a He II transverse proximity effect in the average transmission profile around 20 foreground quasars and by cutting on the transverse separation we could place a clear constraint on the quasar lifetime of $>$25 Myr. What remains however, is the surprising and to some degree contradictory result that our stacking analysis shows evidence for a long quasar lifetime while among the four strongest foreground quasars which all should exceed the He II UV background by an order of magnitude and are at most 15 Mlyr away from the background sightline only the previously known quasar is associated with a strong He II transmission spike.

We would like to apply our method to an even larger dataset. However, given the capabilities of the current UV space telescopes (*GALEX*, *HST*), the discovery of many new He II sightlines is unlikely and a good fraction of the known sightlines has now been searched for foreground quasars. In the near future, new insight into the He II transverse proximity effect will therefore probably come from dedicated modeling. A first attempt for this is shown in **Figure 4**. We take outputs of a cosmological hydrodynamical simulation computed with the

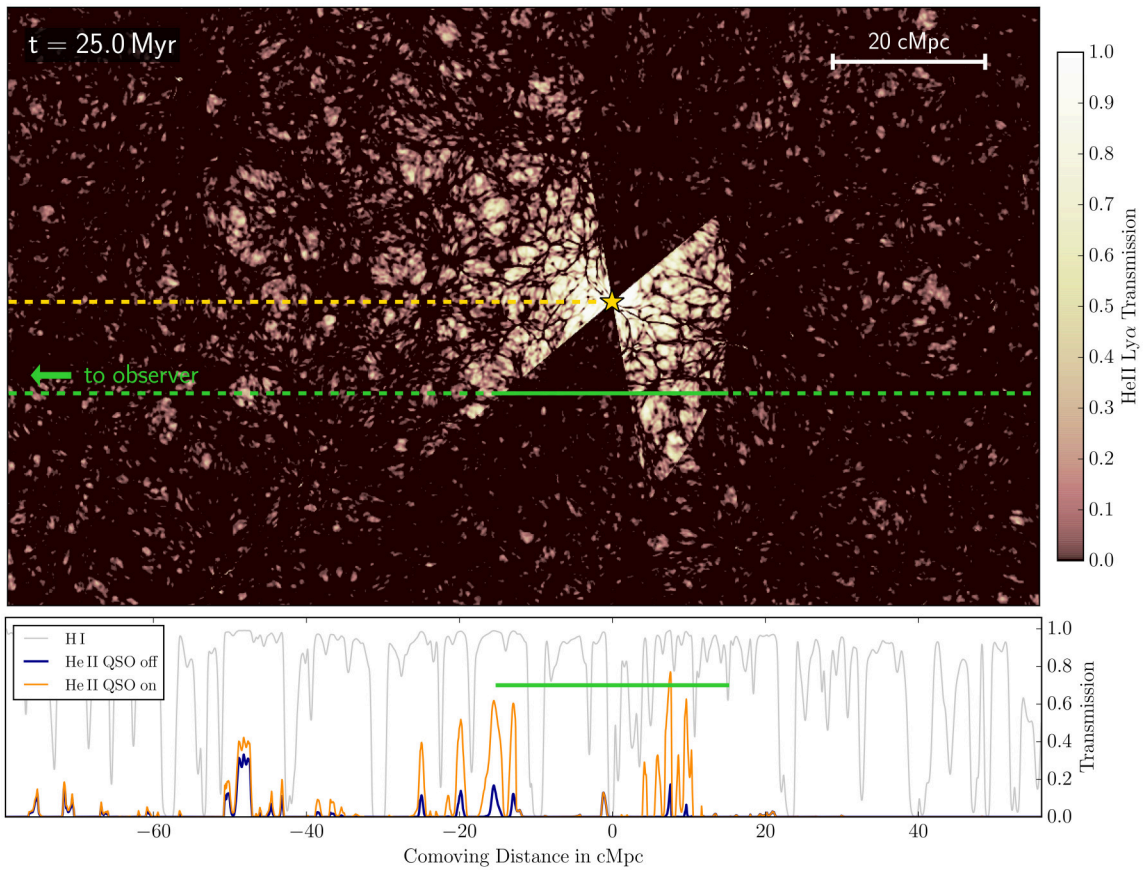

FIGURE 4 | Illustration of our photoionization model we use to investigate the effect of obscuration and finite quasar age. The top panel displays the He II transmission in a slice through the simulation box. It clearly shows the bi-conical emission of the quasar and the parabolic shaped region that can be reached by the quasar emission within the given time. The bottom panel shows the computed hydrogen and helium transmission spectra along a background sightline (green). A strong He II transmission enhancements is visible in regions that are illuminated by the quasar. The solid green bar marks the ±15 cMpc wide region we use to measure the transmission enhancement (Schmidt et al., 2017).

Eulerian grid code Nyx (Almgren et al., 2013; Lukić et al., 2015) and post-process these with a photo-ionization model that simulates a single bright foreground quasar. In this model we can explicitly vary quasar age and emission geometry. The case shown in **Figure 4** is matched in quasar luminosity and sightline geometry to the Q 0302−003 $z = 3.05$ foreground quasar. We chose a classical bi-conical emission geometry with a half-opening angle of $\alpha = 60^\circ$, therefore illuminating 50% of the sky. The quasar is inclined by 20° and assumed to be 25 Myr old. For an observer on Earth, the low redshift parts of the background sightline appears to be illuminated first while the quasar radiation arrive at successively later times at higher redshifts. For a given quasar age, the illuminated region has a parabolic shape, open toward the observer and with the quasar at the focus. The finite quasar age limits the extend of the illuminated region toward high redshifts (larger comoving distance, right side). This is well visible in the top panel of **Figure 4** which shows the simulated He II transmission in a thin slice through the simulation. The bottom panel clearly shows the He II transverse proximity effect along the background sightline and the substantially enhanced transmission compared to the the effect of the $\Gamma_{\rm UVB}^{\rm HeII} \approx 1 \times 10^{-15}\,{\rm s}^{-1}$ UV background alone, but also the effect of obscuration and finite quasar age.

With these models, we intent to investigate the combined effect of quasar obscuration and finite quasar age on the expected He II transmission, compare them to the observed He II spectra associated with the strongest foreground quasars and infer their age and obscuration properties. It is obvious that due to the random quasar orientation any constraints will only be of probabilistic nature and our endeavor will probably require a large Monte Carlo analysis and sophisticated statistical methods. However, given the high expected photoionization rate of the foreground quasars, it should still be possible to rule out certain parts of the parameter space and give insights if a reference model with e.g., 50% obscuration and 25 Myr lifetime is actually consistent with our observations and the non-detection of strong transmission peaks for the strongest foreground quasars.

AUTHOR CONTRIBUTIONS

This work is part of the Ph.D. project of TS under supervision of JH and GW. GW is responsible for the He II FUV spectra. JP and NC provided optical observational data and data reduction tools. Cosmological hydrodynamical simulations were provided by ZL and JO.

FUNDING

GW has been supported by the Deutsches Zentrum für Luft- und Raumfahrt (DLR) under contracts 50 OR 1317 and 50 OR 1512.

ACKNOWLEDGMENTS

We thank Robert Simcoe for kindly supplying Magellan/Megacam imaging for the SDSS J1237+0126 field. We would like to thank the members of the ENIGMA[1] group at the Max Planck Institute for Astronomy (MPIA) for useful discussions and support.

Based on observations made with the NASA/ESA Hubble Space Telescope, obtained at the Space Telescope Science Institute, which is operated by the Association of Universities for Research in Astronomy, Inc., under NASA contract NAS 5-26555. These observations are associated with programs 11528, 11742, 12033, 12178, 12249, 13013.

The LBT is an international collaboration among institutions in the United States, Italy, and Germany. LBT Corporation partners are: The University of Arizona on behalf of the Arizona Board of Regents; Istituto Nazionale di Astrofisica, Italy; LBT Beteiligungsgesellschaft, Germany, representing the Max-Planck Society, The Leibniz Institute for Astrophysics Potsdam, and Heidelberg University; The Ohio State University, and The Research Corporation, on behalf of The University of Notre Dame, University of Minnesota and University of Virginia.

This paper includes data gathered with the 6.5 m Magellan Telescopes located at Las Campanas Observatory, Chile.

Based in part on observations at Cerro Tololo Inter-American Observatory and Kitt Peak National Observatory, National Optical Astronomy Observatory, which are operated by the Association of Universities for Research in Astronomy (AURA) under a cooperative agreement with the National Science Foundation. The authors are honored to be permitted to conduct astronomical research on Iolkam Du'ag (Kitt Peak), a mountain with particular significance to the Tohono O'odham. Based on observations collected at the European Organization for Astronomical Research in the Southern Hemisphere under ESO programmes 088.A-0835(B), 090.A-0664(B), 094.A-0500(A), 094.A-0782(A).

Based on observations collected at the Centro Astronómico Hispano Alemán (CAHA) at Calar Alto, operated jointly by the Max-Planck Institut für Astronomie and the Instituto de Astrofísica de Andalucía (CSIC).

Some of the data presented herein were obtained at the W. M. Keck Observatory, which is operated as a scientific partnership among the California Institute of Technology, the University of California and the National Aeronautics and Space Administration. The Observatory was made possible by the generous financial support of the W. M. Keck Foundation. The authors wish to recognize and acknowledge the very significant cultural role and reverence that the summit of Mauna Kea has always had within the indigenous Hawaiian community. We are most fortunate to have the opportunity to conduct observations from this mountain.

Funding for SDSS-III has been provided by the Alfred P. Sloan Foundation, the Participating Institutions, the National Science Foundation, and the U.S. Department of Energy Office of Science. The SDSS-III web site is http://www.sdss3.org/. SDSS-III is managed by the Astrophysical Research Consortium for the Participating Institutions of the SDSS-III Collaboration including the University of Arizona, the Brazilian Participation Group, Brookhaven National Laboratory, Carnegie Mellon

[1] http://enigma.physics.ucsb.edu/

University, University of Florida, the French Participation Group, the German Participation Group, Harvard University, the Instituto de Astrofisica de Canarias, the Michigan State/Notre Dame/JINA Participation Group, Johns Hopkins University, Lawrence Berkeley National Laboratory, Max Planck Institute for Astrophysics, Max Planck Institute for Extraterrestrial Physics, New Mexico State University, New York University, Ohio State University, Pennsylvania State University, University of Portsmouth, Princeton University, the Spanish Participation Group, University of Tokyo, University of Utah, Vanderbilt University, University of Virginia, University of Washington, and Yale University.

REFERENCES

Alam, S., Albareti, F. D., Allende Prieto, C., Anders, F., Anderson, S. F., Anderton, T., et al. (2015). The eleventh and twelfth data releases of the sloan digital sky survey: final data from SDSS-III. *Astrophys. J. Suppl.* 219:12. doi: 10.1088/0067-0049/219/1/12

Almgren, A. S., Bell, J. B., Lijewski, M. J., Lukić, Z., and Van Andel, E. (2013). Nyx: a massively parallel AMR code for computational cosmology. *Astrophys. J.* 765:39. doi: 10.1088/0004-637X/765/1/39

Antonucci, R. (1993). Unified models for active galactic nuclei and quasars. *Ann. Rev. Astron. Astrophys.* 31, 473–521. doi: 10.1146/annurev.aa.31.090193.002353

Assef, R. J., Stern, D., Kochanek, C. S., Blain, A. W., Brodwin, M., Brown, M. J. I., et al. (2013). Mid-infrared selection of active galactic nuclei with the wide-field infrared survey explorer. II. Properties of WISE-selected active galactic nuclei in the NDWFS Boötes field. *Astrophys. J.* 772:26. doi: 10.1088/0004-637X/772/1/26

Bolton, J. S., Haehnelt, M. G., Viel, M., and Carswell, R. F. (2006). Spatial fluctuations in the spectral shape of the ultraviolet background at $2 < z < 3$ and the reionization of helium. *Month. Notices RAS* 366, 1378–1390. doi: 10.1111/j.1365-2966.2006.09927.x

Brusa, M., Civano, F., Comastri, A., Miyaji, T., Salvato, M., Zamorani, G., et al. (2010). The XMM-Newton wide-field survey in the cosmos field (XMM-COSMOS): demography and multiwavelength properties of obscured and unobscured luminous active galactic nuclei. *Astrophys. J.* 716, 348–369. doi: 10.1088/0004-637X/716/1/348

Buzzoni, B., Delabre, B., Dekker, H., Dodorico, S., Enard, D., Focardi, P., et al. (1984). The ESO faint object spectrograph and camera (EFOSC). *Messenger* 38, 9–13.

Compostella, M., Cantalupo, S., and Porciani, C. (2013). The imprint of inhomogeneous He II reionization on the H I and He II Lyα forest. *Month. Notices RAS* 435, 3169–3190. doi: 10.1093/mnras/stt1510

Compostella, M., Cantalupo, S., and Porciani, C. (2014). AGN-driven helium reionization and the incidence of extended He III regions at redshift $z > 3$. *Month. Notices RAS* 445, 4186–4196. doi: 10.1093/mnras/stu2035

Davies, F. B., Furlanetto, S. R., and Dixon, K. L. (2017). A self-consistent 3D model of fluctuations in the helium-ionizing background. *Month. Notices RAS* 465, 2886–2894. doi: 10.1093/mnras/stw2868

Dawson, K. S., Schlegel, D. J., Ahn, C. P., Anderson, S. F., Aubourg, É., Bailey, S., et al. (2013). The Baryon oscillation spectroscopic survey of SDSS-III. *Astron. J.* 145:10. doi: 10.1088/0004-6256/145/1/10

DiPompeo, M. A., Bovy, J., Myers, A. D., and Lang, D. (2015). Quasar probabilities and redshifts from WISE mid-IR through GALEX UV photometry. *Month. Notices RAS* 452, 3124–3138. doi: 10.1093/mnras/stv1562

Eisenstein, D. J., Weinberg, D. H., Agol, E., Aihara, H., Allende Prieto, C., Anderson, S. F., et al. (2011). SDSS-III: massive spectroscopic surveys of the distant universe, the milky way, and extra-solar planetary systems. *Astron. J.* 142:72. doi: 10.1088/0004-6256/142/3/72

Elvis, M. (2000). A structure for quasars. *Astrophys. J.* 545, 63–76. doi: 10.1086/317778

Faucher-Giguère, C.-A., Lidz, A., Zaldarriaga, M., and Hernquist, L. (2009). A new calculation of the ionizing background spectrum and the effects of He II reionization. *Astrophys. J.* 703, 1416–1443. doi: 10.1088/0004-637X/703/2/1416

Furlanetto, S. R., and Dixon, K. L. (2010). Large-scale fluctuations in the He II Lyα forest and He II reionization. *Astrophys. J.* 714, 355–366. doi: 10.1088/0004-637X/714/1/355

Furlanetto, S. R., and Lidz, A. (2011). Constraints on quasar lifetimes and beaming from the He II Lyα forest. *Astrophys. J.* 735:117. doi: 10.1088/0004-637X/735/2/117

Furlanetto, S. R., and Oh, S. P. (2008). The history and morphology of helium reionization. *Astrophys. J.* 681, 1–17. doi: 10.1086/588546

Giallongo, E., Ragazzoni, R., Grazian, A., Baruffolo, A., Beccari, G., de Santis, C., et al. (2008). The performance of the blue prime focus large binocular camera at the large binocular telescope. *Astron. Astrophys.* 482, 349–357. doi: 10.1051/0004-6361:20078402

Gunn, J. E., and Peterson, B. A. (1965). On the density of neutral hydrogen in intergalactic space. *Astrophys. J.* 142, 1633–1641. doi: 10.1086/148444

Haardt, F., and Madau, P. (2012). Radiative transfer in a clumpy universe. IV. New synthesis models of the cosmic UV/X-ray background. *Astrophys. J.* 746:125. doi: 10.1088/0004-637X/746/2/125

Heap, S. R., Williger, G. M., Smette, A., Hubeny, I., Sahu, M. S., Jenkins, E. B., et al. (2000). STIS observations of HE II Gunn-Peterson absorption toward Q0302-003. *Astrophys. J.* 534, 69–89. doi: 10.1086/308719

Jakobsen, P., Jansen, R. A., Wagner, S., and Reimers, D. (2003). Caught in the act: a helium-reionizing quasar near the line of sight to Q0302-003. *Astron. Astrophys.* 397, 891–898. doi: 10.1051/0004-6361:20021579

Khrykin, I. S., Hennawi, J. F., McQuinn, M., and Worseck, G. (2016). The He II proximity effect and the lifetime of quasars. *Astrophys. J.* 824:133. doi: 10.3847/0004-637X/824/2/133

Le Fèvre, O., Saisse, M., Mancini, D., Brau-Nogue, S., Caputi, O., Castinel, L., et al. (2003). "Commissioning and performances of the VLT-VIMOS instrument," in *Instrument Design and Performance for Optical/Infrared Ground-based Telescopes, Volume 4841 of Proceedings of SPIE*, eds M. Iye and A. F. M. Moorwood, 1670–1681. Available online at: http://adsabs.harvard.edu/abs/2003SPIE.4841.1670L

Lukić, Z., Stark, C. W., Nugent, P., White, M., Meiksin, A. A., and Almgren, A. (2015). The Lyman α forest in optically thin hydrodynamical simulations. *Month. Notices RAS* 446, 3697–3724. doi: 10.1093/mnras/stu2377

Lusso, E., Hennawi, J. F., Comastri, A., Zamorani, G., Richards, G. T., Vignali, C., et al. (2013). The obscured fraction of active galactic nuclei in the XMM-COSMOS survey: a spectral energy distribution perspective. *Astrophys. J.* 777:86. doi: 10.1088/0004-637X/777/2/86

Madau, P., and Meiksin, A. (1994). The He II Lyman-alpha opacity of the universe. *Astrophys. J. Lett.* 433, L53–L56. doi: 10.1086/187546

Marchesi, S., Lanzuisi, G., Civano, F., Iwasawa, K., Suh, H., Comastri, A., et al. (2016). The chandra COSMOS-legacy survey: source X-ray spectral properties. *Astrophys. J.* 830:100. doi: 10.3847/0004-637X/830/2/100

McQuinn, M. (2009). The implications of Gunn-Peterson troughs in the He II Lyα forest. *Astrophys. J. Lett.* 704, L89–L92. doi: 10.1088/0004-637X/704/2/L89

Meiksin, A., and Tittley, E. R. (2012). The impact of helium reionization on the structure of the intergalactic medium. *Month. Notices RAS* 423, 7–25. doi: 10.1111/j.1365-2966.2011.20380.x

Miralda-Escudé, J., Haehnelt, M., and Rees, M. J. (2000). Reionization of the inhomogeneous universe. *Astrophys. J.* 530, 1–16. doi: 10.1086/308330

Pâris, I., Petitjean, P., Ross, N. P., Myers, A. D., Aubourg, É., Streblyanska, A., et al. (2016). The sloan digital sky survey quasar catalog: twelfth data release. ArXiv e-prints.

Planck Collaboration, Adam, R., Aghanim, N., Ashdown, M., Aumont, J., Baccigalupi, C., et al. (2016). Planck intermediate results. XLVII. Planck constraints on reionization history. *Astron. Astrophys.* 596:A108. doi: 10.1051/0004-6361/201628897

Reimers, D., Kohler, S., Wisotzki, L., Groote, D., Rodriguez-Pascual, P., and Wamsteker, W. (1997). Patchy intergalactic He II absorption in HE 2347-4342. II. The possible discovery of the epoch of He-reionization. *Astron. Astrophys.* 327, 890–900.

Richards, G. T., Myers, A. D., Peters, C. M., Krawczyk, C. M., Chase, G., Ross, N. P., et al. (2015). Bayesian high-redshift quasar classification from optical and Mid-IR photometry. *Astrophys. J. Suppl.* 219:39. doi: 10.1088/0067-0049/219/2/39

Schmidt, T. M., Worseck, G., Hennawi, J. F., Prochaska, J. X., and Crighton, N. H. M. (2017). Statistical detection of the HeII transverse proximity effect: evidence for sustained quasar activity for >25 million years. *Astrophys. J.* 847:81. doi: 10.3847/1538-4357/aa83ac

Speziali, R., Di Paola, A., Giallongo, E., Pedichini, F., Ragazzoni, R., Testa, V., et al. (2008). "The Large Binocular Camera: description and performances of the first binocular imager," in *Ground-based and Airborne Instrumentation for Astronomy II, Volume 7014 of Proceedings of the SPIE*, eds I. S. McLean and M. M. Casali. Available online at: http://adsabs.harvard.edu/abs/2008SPIE.7014E..4TS

Stern, D., Assef, R. J., Benford, D. J., Blain, A., Cutri, R., Dey, A., et al. (2012). Mid-infrared selection of active galactic nuclei with the wide-field infrared survey explorer. I. Characterizing WISE-selected active galactic nuclei in COSMOS. *Astrophys. J.* 753:30. doi: 10.1088/0004-637X/753/1/30

Worseck, G., Prochaska, J. X., Hennawi, J. F., and McQuinn, M. (2016). Early and extended helium reionization over more than 600 million years of cosmic time. *Astrophys. J.* 825:144. doi: 10.3847/0004-637X/825/2/144

Worseck, G., Prochaska, J. X., McQuinn, M., Dall'Aglio, A., Fechner, C., Hennawi, J. F., et al. (2011). The end of helium reionization at z ˜= 2.7 inferred from cosmic variance in HST/COS He II Lyα absorption spectra. *Astrophys. J. Lett.* 733:L24. doi: 10.1088/2041-8205/733/2/L24

Wright, E. L., Eisenhardt, P. R. M., Mainzer, A. K., Ressler, M. E., Cutri, R. M., Jarrett, T., et al. (2010). The wide-field infrared survey explorer (WISE): mission description and initial on-orbit performance. *Astron. J.* 140, 1868–1881. doi: 10.1088/0004-6256/140/6/1868

York, D. G., Adelman, J., Anderson, J. E. Jr., Anderson, S. F., Annis, J., Bahcall, N. A., et al. (2000). The sloan digital sky survey: technical summary. *Astron. J.* 120, 1579–1587. doi: 10.1086/301513

Conflict of Interest Statement: The authors declare that the research was conducted in the absence of any commercial or financial relationships that could be construed as a potential conflict of interest.